ELSEVIER

Chemical Engineering Journal 84 (2001) 77–94

Chemical Engineering Journal

www.elsevier.com/locate/cej

Film-pore diffusion modeling and contact time optimization for the adsorption of dyestuffs on pith

Buning Chen, Chi Wai Hui, Gordon McKay*

Department of Chemical Engineering, The Hong Kong University of Science and Technology, Clear Water Bay, Kowloon, Hong Kong, SAR China

Abstract

The sorption of four dyestuffs, namely, Acid Blue 25 (AB25), Acid Red 114 (AR114), Basic Blue 69 (BB69) and Basic Red 22 (BR22) onto bagasse pith has been studied using an agitated batch sorber system. The equilibrium isotherms were determined and kinetic runs were performed over a range of concentrations for each dye and masses of pith. A film-pore diffusion mass transfer model has been developed based on a single effective diffusion coefficient for each system. Error analysis of the experimental and theoretical data indicated relatively large errors at low initial dyestuff concentrations.

In this paper, a contact time optimization methodology of a two-stage batch adsorber system taking minimum contact time as the objective function has been developed. The initial concentration of the second stage and adsorbent weight have been designated as variables. Contact time optimization of a two-stage batch adsorber system has been demonstrated at two different conditions/cases for the adsorption of dyes on pith. The optimization solutions show that there is a significant difference for minimum contact time at different process conditions.

Keywords: Adsorption; Modeling and optimization; Film-pore diffusion; Dyes; Pith

1. Introduction

Adsorption is a physico-chemical wastewater treatment method, which has gained popularity in the wastewater treatment industry because of the high-quality treated effluents it produces. In many cases, these treated effluents can be re-used in a range of processes as good quality water.

Adsorption is the process by which a solid adsorbent can attract a component in water to its surface and form an attachment via a physical or chemical bond, thus removing the component from the fluid phase.

In order to develop an effective and accurate design model for batch, fixed bed and fluidized bed adsorption systems, adsorption kinetics and equilibrium data are two essential basic requirements. Adsorption kinetics show a large dependence on the physical characteristics of the adsorbent material which also influences the adsorption mechanism. Other relevant factors include adsorbate–adsorbent chemical properties and system conditions.

Many adsorption models exist describing the rate and extent of adsorption of a solute on to an adsorbent particle. The main problems are the accuracy of model prediction and the time and methodology to execute the application of the model. There are four main models representations commonly used for describing adsorption with significant mass transfer resistance: (i) the reaction rate approach; (ii) linear driving force expressions for the internal and external mass transport processes; (iii) non-linear driving force expressions; and (iv) reversible or irreversible adsorption. The model applied in the present paper is based on external film mass transfer and pore diffusion.

The pore phase diffusion model pictures the adsorbent particle as consisting of a solid-phase interspersed with very small pores. The adsorbate diffuses into the pores in the fluid phase and adsorption occurs at the internal surfaces. Amundson and coworkers [1–4] obtained analytical solutions on terms of infinite series for linear adsorption isotherms with batch and fixed-bed reactor configurations. Di Giano and Weber [5] and Weber [6] used the same approach to study adsorption in finite and infinite batch systems. In the finite batch system, assumptions of irreversible immobilization and quasi steady-state in the solid-phase were made.

The latter assumption implies that the rate of immobilization of the solute is rapid compared to the motion of the solution front in the solid. The model is suitable only for solutes satisfying the dual criteria of irreversible adsorption and large solid-to-liquid equilibrium solute distributions. The Freundlich isotherm has been used to describe

* Corresponding author. Tel.: +86-852-2358-7130; fax: +86-852-2358-0054.
E-mail address: kemckayg@ust.hk (G. McKay).

1385-8947/01/$ – see front matter
PII: S1385-8947(01)00193-0

Nomenclature

a	$[(1 - C_h)/C_h]^{1/3}$, a simplifying term used in Eq. (1)
B	$(1 - (1/B_i))$, a simplifying term used in Eq. (1)
B_i	Biot number, $\beta_L R/D_{eff}$
C	concentration (mg/dm^3)
C_h	capacity factor, Sq_e/VC_0
d	differential
d_p	particle diameter (cm)
D	diffusivity or diameter (cm^2/s or cm)
ln	natural logarithm
max	maximizing
min	minimizing
N	mass transfer rate (mg/s)
r	particle radius as variable (cm)
R	particle radius (cm)
S	adsorbent weight (mg)
t	time (s)
V	volume of liquid phase (dm^3)
x	$(1 - \eta)^{1/3}$, a simplifying term used in Eq. (1)
Y	solid-phase concentration (mg/g)

Greek letters

β_L	external mass transfer coefficient (cm/s)
ε_p	porous ratio of adsorbent, dimensionless
η	dimensionless solid-phase concentration
μ	tortuosity factor
ρ_s	density of adsorbent particle (mg/cm^3)
τ	dimensionless contact time, $C_0 D_{eff} t/\rho_s q_e R^2$
∂	differential of variable summation

Subscripts

e	equilibrium
eff	effective
L	liquid
max	maximum
min	minimum
p	pore
s	solid or surface
t	time
0	initial
1	first stage
2	second stage

equilibrium behavior on heterogeneous surfaces [7–10]. However, the mathematical exponential format of the Freundlich isotherm renders it unsuitable for the assumption of a pseudo-irreversible isotherm which reaches a monolayer saturation capacity. Although derived to explain reversible adsorption situations, the Langmuir equation can adequately reflect irreversible adsorption systems and is characterized by the 'monolayer plateau' that signifies saturation capacity ([11,12] and McKay and Al Duri [8]). Assuming external mass transfer, pore diffusion and irreversible adsorption, an analytical solution has been obtained for the determination of adsorption rates of single organic solutes in batch tests.

In reality the true mechanism involves external film, pore and surface diffusion apart from sorbate–sorbent interactions. The mathematical models implement assumptions to reduce mathematical complexity and data processing time while optimizing the accuracy of theoretical predictions when compared with experimental data. A film-pore diffusion model has been adopted in this study based on the unreacted shrinking core mass transfer model [13,14]. The adsorption reaction starts at the particle surface forming a reacted zone which move inwards with a defined velocity. Therefore, during the entire reaction time there is an unreacted core, shrinking in size as adsorption proceeds.

Although most industrial applications are based on fixed bed adsorption, many batch-processing industries consider that batch adsorption plant is more suitable to their requirements. Previous studies [15,16] on optimizing multi-stage batch adsorber systems have been based on minimizing the amount of adsorbent and assuming sufficient residence time is allowed for the adsorption system to reach equilibrium or at least 70–80% equilibrium capacity. This approach is suitable for expensive adsorbent such as zeolites, molecular sieves, activated carbon, etc. but optimization based on minimizing the amount of adsorbent, may not always be the main criterion. Due to size and space limitations on congested industrial sites, the treatment capacity of a hatch adsorption plant may be limited. The ability of a batch adsorption plant must then be designed based on the ability of this treatment system to process several batches of process effluent per day; rather than using a minimum quantity of adsorbent and utilizing a maximum contact time to achieve equilibrium saturation.

The systems under investigation in this study are the adsorption of two acid dyes and two basic dyes onto bagasse pith — a waste material from the sugar cane industry. Equilibrium isotherms and agitated batch contact time studies have been performed although the main thrust of the paper is to develop a batch design optimization technique to minimize the contact time for a two-stage batch adsorber system.

2. Theory

A film-pore diffusion model has been applied in the present research to predict the concentration versus time decay curves in batch absorbers. The basic model is based on the unreacted shrinking core mass transfer model, Shrinking-Core Model (SCM) [14]. The SCM model has been applied to several sorption systems successfully, including organics [17–19], dyestuffs [20,21] and metal ions [22–26]. Only the fundamental equations are presented in the following section, the detailed mathematical derivations may be obtained from the cited references in this section.

An assumption of this model is that the adsorption rate is controlled by an external and an internal pore mass transfer

resistance. Diffusion in the pore liquid occurs according to Fick's law [27,28].

A number of solutions to this model have been developed [17,21]. However, since the main objective of the present research is to develop a batch adsorber optimization model, then the simplest SCM model will be adopted, which enables rapid analytical integration of the differential equations. The mathematical methods for performing this integration have been reported previously [29,30]. The integrated form is given by Eq. (1) and the computer program development is simple and involves the solution of Eq. (1) with appropriate structuring and iterations

$$\tau = \frac{1}{6C_h}\left\{\ln\left[\frac{x^3+a}{1+a^3}\right]^{(2B-(1/a))} + \ln\left[\frac{x+a}{1+a}\right]^{3/a}\right\} + \frac{1}{aC_h\sqrt{3}}\left\{\arctan\left[\frac{2-a}{a\sqrt{3}}\right] - \arctan\left[\frac{2x-a}{\sqrt{3}}\right]\right\} \quad (1)$$

3. Materials and experimental techniques

3.1. Materials

3.1.1. Adsorbent

The adsorbent used in this investigation was an Egyptian bagasse pith provided from Abou-Korkas sugar mill, El-Mina, Egypt. The depithing operation was performed in the sugar mill. The moisture content of the bagasse pith was 14.5 ± 10.5%, and it was not subjected to any form of pretreatment prior to use. The pith particles were sieved in the laboratory to obtain a discrete size range of 500–710 μm.

The particles were assumed to be spheres having a diameter given by the arithmetic mean value between respective mesh sizes, i.e. 605 μm. The particles appeared irregularly shaped under a microscope but approximated more closely to spheres than to cylinders or parallel pipes for the size range under investigation.

The Egyptian bagasse pith was subjected to chemical analysis [31] and the results obtained are given in Table 1.

Table 1
Chemical analysis of the bagasse pith

Determination	In %
α-Cellulose	53.7
Pentosan	27.9
Lignin	20.2
Alcohol/benzene solubility	7.5
Ash	6.6

3.1.2. Adsorbates

The adsorbates and their structures used in the experiments are listed below. The dyestuffs were used as the commercial salts.

1. Acid Blue 25 (AB25) (Teflon Blue ANL) CI 62055 was supplied by Bayer.
2. Acid Red 114 (AR114) (Erionyl Red RS) CI 23635 was supplied by Ciba–Geigy.
3. Basic Red 22 (BR22) (Maxilon Red Bl-N) CI 11055 was supplied by Ciba–Geigy.
4. Basic Blue 69 (BB69) (Astrazone Blue FRR) was supplied by Bayer.

No structure is available for this dye. It belongs to the methine class, of which the chromophore is a conjugate chain of carbon atoms terminated by an ammonium group, and in addition, a nitrogen, sulfur, or oxygen atom, or an equivalent unsaturated group. A general structure for the methine class is shown.

AB25

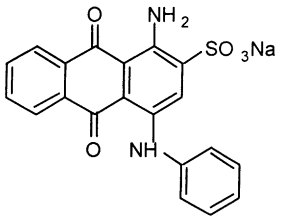

BB69

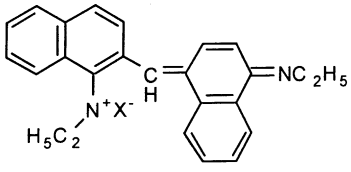

AR114

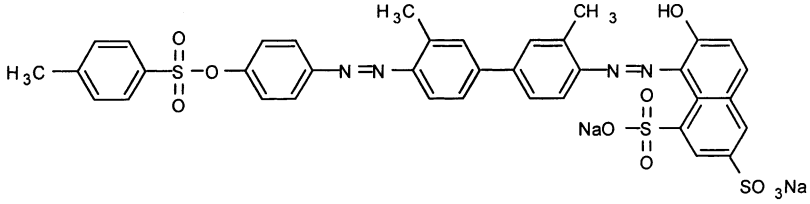

BR22

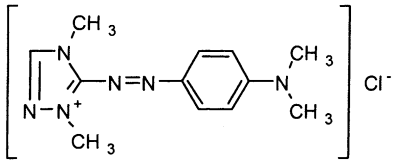

Table 2
Maximum adsorbance wavelength of dyes

Dye	λ_{max} (nm)
AB25	600
AR114	522
BB69	585
BR22	538

Table 3
Langmuir constants of dyes

Dye	K_L (dm^3/g)	a_L (dm^3/mg)	r^2
AB25	0.50	0.023	0.996
AR114	1.1	0.048	0.990
BB69	16.0	0.100	0.995
BR22	18	0.235	0.993

3.2. Analytical techniques

3.2.1. Preparation of calibration curve

The dyes were made up in stock solutions of concentration 1000 ppm and were subsequently diluted to the required concentrations. Calibration curves for each dye were prepared by recording the adsorbance values for a range of known concentrations of dye solution at the wavelength to maximum adsorbance of each dye. This value, λ_{max}, was found from a scan of the dye's spectrum and the values are given in Table 2. These values of λ_{max} were used in all subsequent investigations using these dyes. All measurements were made on a Perkin-Elmer Model 550S Spectrophotometer.

3.3. Experimental

3.3.1. Equilibrium isotherms

Equilibrium studies were carried out to determine the adsorption capacities for the four dyes onto bagasse pith. The isotherms were determined by agitating 0.25 g pith with 0.05 dm^3 dye solution, having concentrations from 10 to 1000 mg/dm^3, for 5 days at a constant temperature of $18 \pm 2^\circ$C.

3.3.2. Batch adsorber studies

The adsorber vessel used for the contact time experiments was based on the standard mixing tank configuration.

A 2 dm^3 glass beaker of i.d. 0.13 m was used and a volume of 17 dm^3 of solution. A six-blade, flat, stainless-steel impeller provided good mixing in the vessel. A Heidolph type 5011 variable-speed motor was used to drive the impeller using a 0.013 m diameter aluminum shaft. Eight baffles were spaced evenly around the vessel circumference to prevent the formation of a vortex and the consequential reduction in relative motion between liquid and solid particles, and power losses due to air entertainment at the impeller. The baffles used were flat strips of aluminum 0.2 m long and 0.013 m wide. The mixing characteristics and performance of this agitation configuration have been described and discussed previously [32–35].

Kinetic data were collected for a series of system parameters. Samples were extracted at selected time interval (up to a maximum of 48 h) using a 0.05 dm^3 syringe. The concentration was determined and the results were recorded as a concentration versus time.

3.3.2.1. Equilibrium isotherms. Equilibrium data are important in developing an effective and accurate model. Under equilibrium situations, the distribution of dye between the adsorbent (pith) and the dye solution is important since the capacity of the adsorbent for the dyestuff can be established. Langmuir and Freundlich isotherms were tested as the equilibrium isotherms. The equation of the Langmuir isotherms is given in Eq. (2) and the Langmuir data were found to have the highest correlation coefficients

$$Y_{e,t} = \frac{K_L C_{e,t}}{1 + a_L C_{e,t}} \quad (2)$$

where K_L and a_L are the Langmuir constants. The Langmuir constants are shown in Table 3 and the equilibrium isotherms of the four dyes are shown in Figs. 1 and 2. The particle size and temperature are kept at 500–710 μm and 20°C, respectively.

Fig. 1 shows that AB25 has an adsorption capacity (i.e. equilibrium solid-phase concentration) of 17.5 ± 0.5 mg/g while that of AR114 is 20.0 ± 0.5 mg/g. The adsorption capacities of BB69 and BR22 in Fig. 2 are 152 ± 5 and 75 ± 2 mg/g, respectively. From the data, it can be clearly seen that the basic dyes have much greater adsorption capacities (i.e. a greater affinity for the pith) than the acid dyes. This is due to the nature of pith.

The structure of pith is cellulose-based and the surface of cellulose becomes negatively charged when in contact with water. Most dyes ionize in solution, many being salts of sulphonic or carboxylic acid, while others contain acidic phenolic groups. AB25 is an example, which ionizes to an anionic colored component D^- and an Na^+ cation. The approach of the acidic dye anion towards the negatively charged pith surface will suffer coulombic repulsion. However, BB69 is an example of a dye which ionizes to give a colored cationic dyebase and this will undergo attraction when approaching the anionic pith structure. Therefore, the adsorption capacities or the affinity of dyes towards pith is greater for basic dyes.

Lignin is also present in pith in considerable amounts. The composition of pith is 60% cellulose and 20% lignin. The lignins in pith are mainly derived from coniferyl alcohol. The negative charges of hydroxylic groups in lignin exert a considerable repulsive force on approaching anions. Therefore, basic dyes have greater affinity towards pith when compared with acidic dyes.

Based on the above information, it is expected that basic dyes have a stronger adsorption affinity for pith. This can

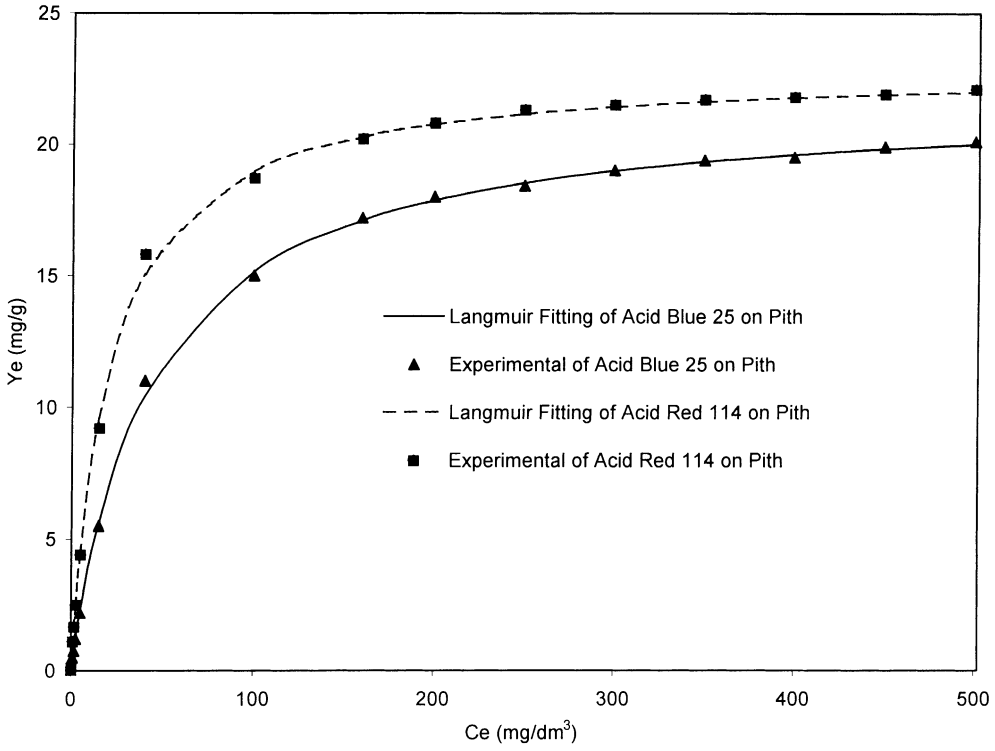

Fig. 1. Langmuir isotherms for AB25 and AR114 on pith.

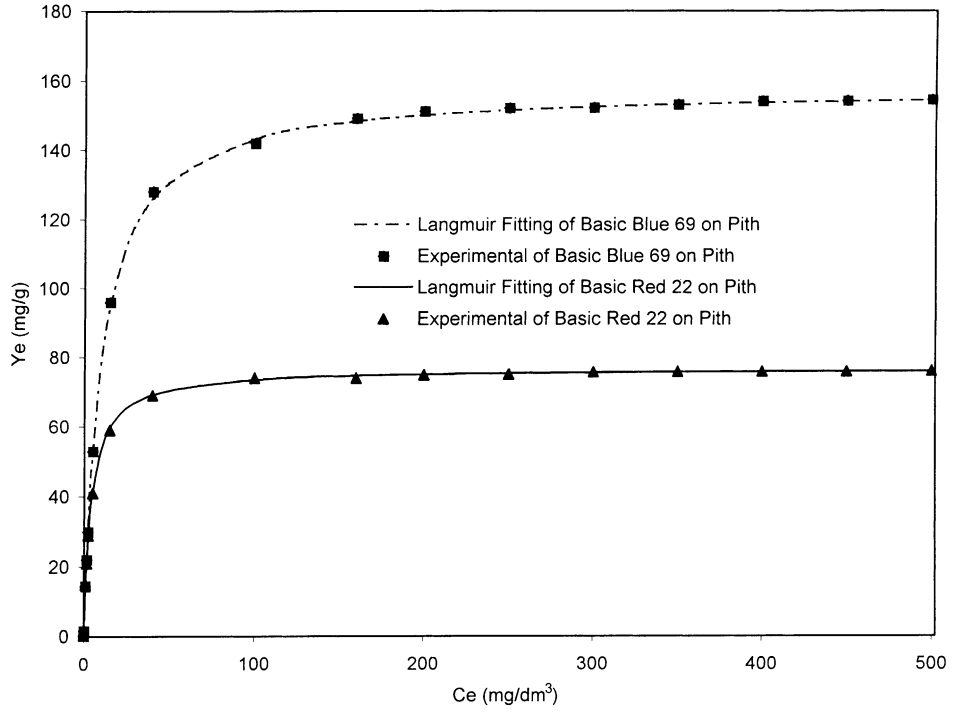

Fig. 2. Langmuir isotherms of BB69 and BR22 on pith.

Table 4
Relative magnitude (K_L/a_L) of equilibrium uptake

Dye	K_L/a_L
AB25	21.7
AR114	22.9
BB69	157
BR22	76.6

be observed by comparing the relative magnitudes of the equilibrium uptake for the dyes presented as K_L/a_L values in Table 4. The larger the value of K_L/a_L, the stronger the adsorption affinity.

3.3.2.2. Mass transfer model 1. This model is based on optimizing all the experimental results for different masses and different concentrations and determining the single best fit β_L and the single best fit D_{eff} for each of the four dye–pith experimental systems. The values of β_L and D_{eff} are shown in Tables 5 and 6 for the two acid dyes and the two basic dyes, respectively. The effective diffusivities for the basic dyes are an order of magnitude greater than the diffusivities of acid dyes. Examples of model 1 fits to experimental data are shown in Figs. 3–5. Visual inspection of these four figures indicates good fits between experimental data and theoretical curves in most cases except for high pith masses and low initial dye concentrations. This observation is confirmed by the percentage error values in Tables 5 and 6. An average error value of 5% represents a minor deviation and an average error value over 10% represents a significant deviation. There are three minor deviations and three significant deviations.

3.3.2.3. Mass transfer model 2. This model is based on optimizing one set of data, i.e. one concentration versus time decay curve to find the best fit individual D_{eff} while maintaining constant for each dye–pith system.

The deviations can be explained by the full expression for effective diffusivity

$$D_{eff} = D_p + \rho_s D_s \frac{\delta Y}{\delta C} \quad (3)$$

where D_p is the pore diffusion coefficient, D_s the solid-phase diffusion coefficient and $\delta Y/\delta C$ is the slope of the equilibrium isotherm.

The pore diffusion coefficient, D_p is a constant. However, the solid-phase diffusion coefficient, D_s, is a function of temperature and the equilibrium solid-phase concentration. The slope of the equilibrium isotherm is determined at the point where the equilibrium isotherm and the operating line intersect at equilibrium and at the coordinates $C_{e,t}$, $Y_{e,t}$ for time dependent surface concentrations.

At high initial concentrations or low masses in Tables 5 and 6, the intersections of the equilibrium isotherm and the operating line lie towards the right of the isotherm. The slope of the equilibrium isotherm is very small and, therefore, the

Table 5
Prediction results of AB25 and AR114 on pith by using the film-pore diffusion model and the searched best system D_{eff} values

System		S (g)	C_0 (mg/dm^3)	β_L (cm/s)	D_{eff} (cm^2/s)	Average error (%)
Adsorbate	Adsorbent					
AB25	Pith	3.4	100	1.75E−3	5.27E−7	2.25
		2.55	100	1.75E−3	5.27E−7	1.47
		2.125	100	1.75E−3	5.27E−7	1.08
		1.70	100	1.75E−3	5.27E−7	0.85
		1.275	100	1.75E−3	5.27E−7	0.45
		0.85	100	1.75E−3	5.27E−7	0.23
		3.4	26	1.75E−3	5.27E−7	6.61
		3.4	53	1.75E−3	5.27E−7	2.67
		3.4	79	1.75E−3	5.27E−7	0.77
		3.4	100	1.75E−3	5.27E−7	0.69
		3.4	129	1.75E−3	5.27E−7	1.35
		3.4	166	1.75E−3	5.27E−7	1.71
AR114	Pith	3.4	100	7.50E−4	7.35E−7	1.38
		2.55	100	7.50E−4	7.35E−7	0.96
		2.125	100	7.50E−4	7.35E−7	0.56
		1.70	100	7.50E−4	7.35E−7	0.45
		1.275	100	7.50E−4	7.35E−7	0.22
		0.85	100	7.50E−4	7.35E−7	0.18
		3.4	25	7.50E−4	7.35E−7	7.54
		3.4	50	7.50E−4	7.35E−7	4.36
		3.4	75	7.50E−4	7.35E−7	1.84
		3.4	100	7.50E−4	7.35E−7	0.46
		3.4	125	7.50E−4	7.35E−7	0.67
		3.4	150	7.50E−4	7.35E−7	1.07

Table 6
Prediction results of BB69 and BR22 on pith by using the film-pore diffusion model and the searched best system D_{eff} values

System		S (g)	C_0 (mg/dm^3)	β_L (cm/s)	D_{eff} (cm^2/s)	Average error (%)
Adsorbate	Adsorbent					
BB69	Pith	2.55	200	4.30E−3	8.60E−6	6.12
		2.125	200	4.30E−3	8.60E−6	2.17
		1.70	200	4.30E−3	8.60E−6	1.48
		1.275	200	4.30E−3	8.60E−6	2.50
		0.85	200	4.30E−3	8.60E−6	1.36
		0.425	200	4.30E−3	8.60E−6	1.07
		1.7	300	4.30E−3	8.60E−6	3.71
		1.7	250	4.30E−3	8.60E−6	3.53
		1.7	200	4.30E−3	8.60E−6	3.03
		1.7	150	4.30E−3	8.60E−6	1.39
		1.7	100	4.30E−3	8.60E−6	12.56
		1.7	50	4.30E−3	8.60E−6	31.71
BR22	Pith	2.55	200	3.46E−3	2.90E−6	4.65
		2.125	200	3.46E−3	2.90E−6	2.83
		1.70	200	3.46E−3	2.90E−6	1.13
		1.275	200	3.46E−3	2.90E−6	0.54
		0.85	200	3.46E−3	2.90E−6	0.39
		0.425	200	3.46E−3	2.90E−6	0.79
		1.7	300	3.46E−3	2.90E−6	0.65
		1.7	250	3.46E−3	2.90E−6	0.85
		1.7	200	3.46E−3	2.90E−6	1.77
		1.7	150	3.46E−3	2.90E−6	1.99
		1.7	100	3.46E−3	2.90E−6	3.54
		1.7	50	3.46E−3	2.90E−6	20.89

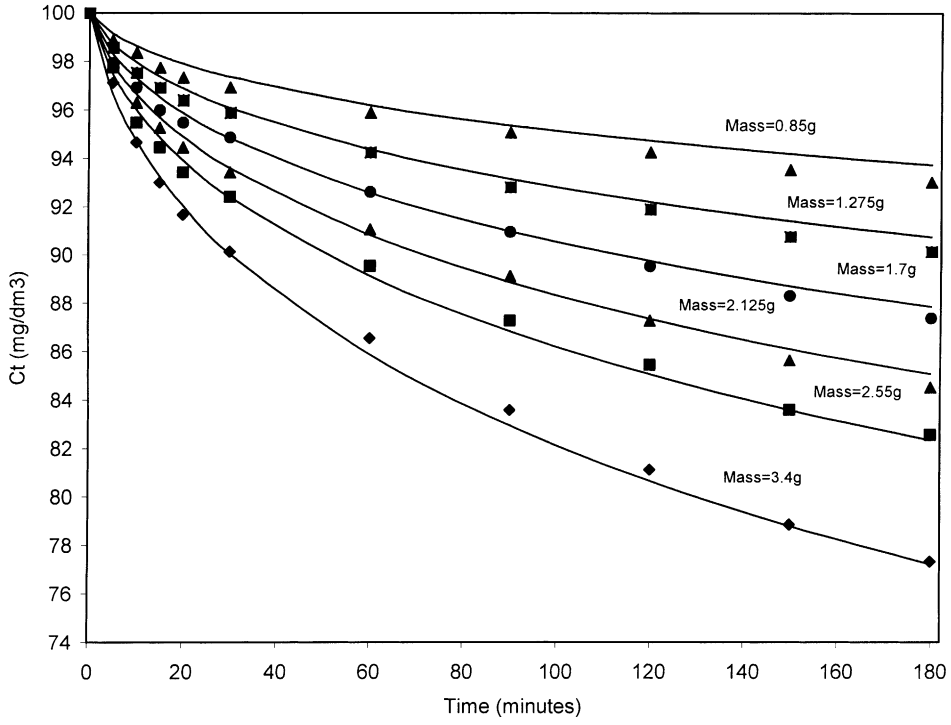

Fig. 3. Effect of pith mass for AR114 on pith by using the searched best system D_{eff} values.

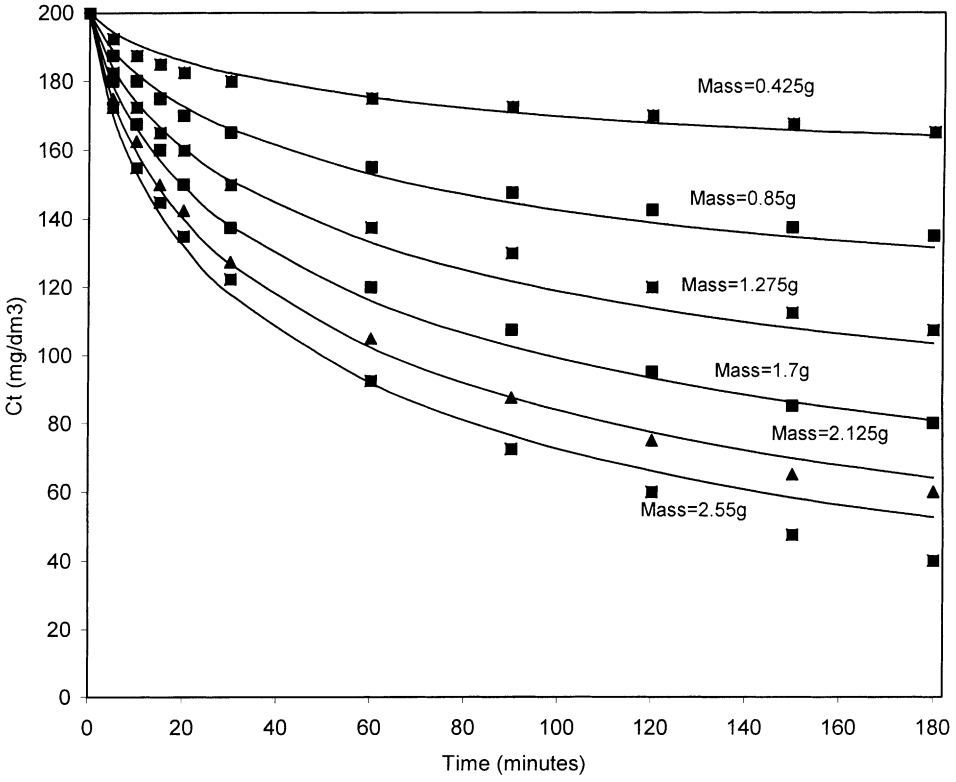

Fig. 4. Effect of pith mass for BB69 on pith by using the searched best system D_{eff} values.

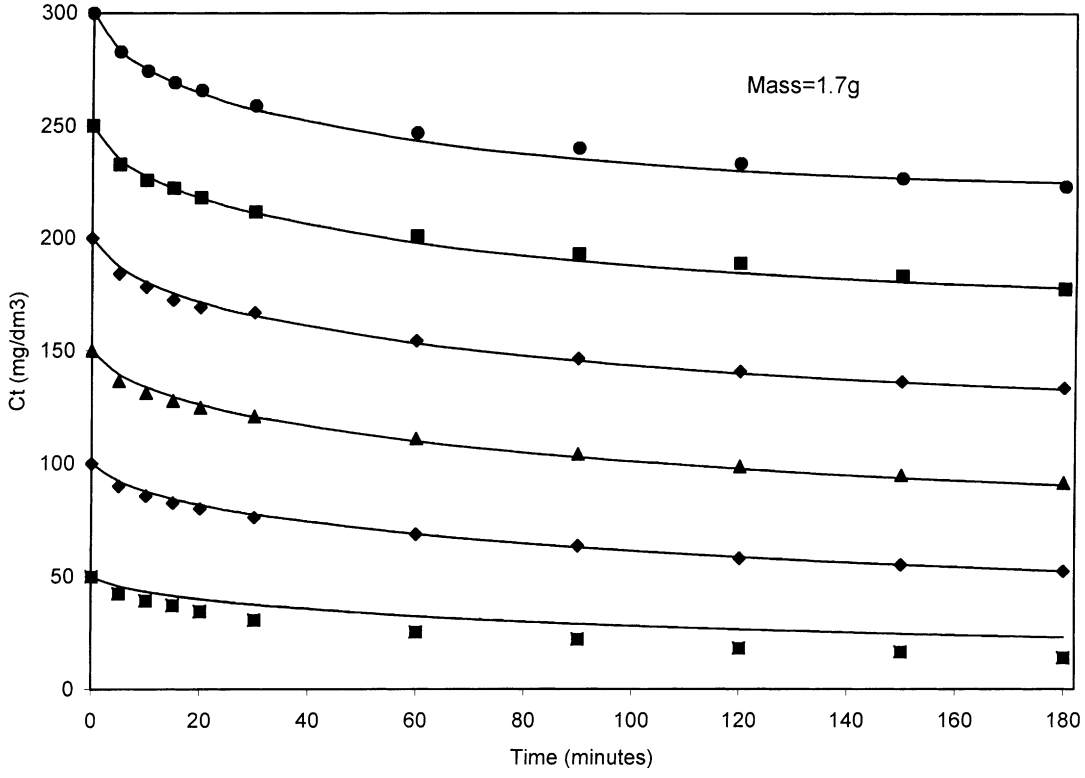

Fig. 5. Effect of initial concentration for BR22 on pith by using the searched best system D_{eff} values.

whole term is negligible. This makes D_{eff} gets closer to a constant, D_p.

However, at low initial concentrations, the intersections lie towards the left of the isotherm. The slope is very large and D_{eff} gets closer to $\rho_s D_s(\delta Y/\delta C)$.

Therefore, if a best fit D_{eff} has to be found for a system, it can only fit the data sets with high initial concentrations. This explains the deviations observed for different initial dye concentrations. The trend in D_{eff} with pith mass is not so clear and D_{eff} values are relatively constant with mass. The D_{eff} values for the two acid dyes and BR22 increase slightly with increasing pith mass. However, the D_{eff} values for BB69, which has by far the highest sorption capacity, show a slightly decreasing trend with mass. This suggests that dye mobility on the pith surface is retarded at high capacity loading.

Apart from looking at the equilibrium isotherm, the above deviations can be observed in the tables of individual D_{eff}. When looking at the values, it was observed that the data sets in which the correlated results deviated a lot from the experimental data have D_{eff} very much different from other data sets. For example, in BB69, the deviations occurred at $C_0 = 50$ and 100 mg/dm^3. Using the 'best fit' individual D_{eff} results in only one significant deviation and two minor deviations with average error percentages of 5.30 and 6.44 are observed in Tables 7 and 8. The quality of the fits between the theoretical concentration versus time decay curves and the experimental data points are shown in Figs. 6–9.

In optimizing the data sets to get a D_{eff}, it is observed that when increasing the initial slope of the correlated results in increased. At the start, external mass transfer takes place and controls the initial adsorption rate. Therefore increasing β_L increases the external mass transfer rate, and hence, the initial slope of the correlated results.

For the same model and same dye, β_L, is the same in all situations because the external mass transfer is not affected by the initial concentration of dye and the mass of adsorbent. External mass transfer occurs across the boundary layer film surrounding the adsorbent particle and therefore depends on liquid density, viscosity, temperature, adsorbent particle size and degree of agitation. Providing the concentration of particles in the solution is low then adsorbent mass does not affect external mass transfer. Similarly, providing sorbate concentrations are low then solution viscosity and density will remain similar to those of water and external mass transfer will be unaffected.

3.3.3. The relationship between D_{eff}, C_0 and S

Individual values of D_{eff} with individual C_0 or S values is a major restriction to the use of this model to general batch sorber design and in particular to multistage optimization when differentiation of an analytical function is much easier than optimizing a series of discrete functions. Therefore, it

Table 7
Prediction results of AB25 and AR114 on pith by using the film-pore diffusion model and the searched best individual D_{eff} values

System		S (g)	C_0 (mg/dm^3)	β_L (cm/s)	D_{eff} (cm^2/s)	Average error (%)
Adsorbate	Adsorbent					
AB25	Pith	3.4	100	1.75E−3	3.19E−7	0.66
		2.55	100	1.75E−3	3.35E−7	0.38
		2.125	100	1.75E−3	3.53E−7	0.27
		1.70	100	1.75E−3	3.58E−7	0.15
		1.275	100	1.75E−3	4.08E−7	0.09
		0.85	100	1.75E−3	4.23E−7	0.08
		3.4	26	1.75E−3	1.05E−6	3.30
		3.4	53	1.75E−3	7.59E−7	0.89
		3.4	79	1.75E−3	6.00E−7	0.52
		3.4	100	1.75E−3	4.41E−7	0.47
		3.4	129	1.75E−3	3.58E−7	0.48
		3.4	166	1.75E−3	3.16E−7	0.21
AR114	Pith	3.4	100	7.50E−4	5.69E−7	0.29
		2.55	100	7.50E−4	5.60E−7	0.28
		2.125	100	7.50E−4	6.28E−7	0.25
		1.70	100	7.50E−4	6.42E−7	0.23
		1.275	100	7.50E−4	6.93E−7	0.17
		0.85	100	7.50E−4	7.89E−7	0.16
		3.4	25	7.50E−4	1.33E−6	6.44
		3.4	50	7.50E−4	1.27E−6	1.65
		3.4	75	7.50E−4	9.99E−7	0.61
		3.4	100	7.50E−4	7.77E−7	0.43
		3.4	125	7.50E−4	6.32E−7	0.20
		3.4	150	7.50E−4	5.85E−7	0.34

Table 8
Prediction results of BB69 and BR22 on pith by using the film-pore diffusion model and the searched best individual D_{eff} values

System		S (g)	C_0 (mg/dm^3)	β_L (cm/s)	D_{eff} (cm^2/s)	Average error (%)
Adsorbate	Adsorbent					
BB69	Pith	2.55	200	4.30E−3	9.83E−6	5.30
		2.125	200	4.30E−3	9.34E−6	2.15
		1.70	200	4.30E−3	7.98E−6	1.38
		1.275	200	4.30E−3	6.92E−6	1.32
		0.85	200	4.30E−3	7.14E−6	0.80
		0.425	200	4.30E−3	7.56E−6	1.01
		1.7	300	4.30E−3	6.03E−6	0.58
		1.7	250	4.30E−3	6.26E−6	0.94
		1.7	200	4.30E−3	6.59E−6	1.07
		1.7	150	4.30E−3	9.32E−6	1.13
		1.7	100	4.30E−3	1.59E−5	3.21
		1.7	50	4.30E−3	3.78E−5	12.50
BR22	Pith	2.55	200	3.46E−3	1.94E−6	0.32
		2.125	200	3.46E−3	2.16E−6	0.23
		1.70	200	3.46E−3	2.35E−6	0.54
		1.275	200	3.46E−3	2.73E−6	0.47
		0.85	200	3.46E−3	3.03E−6	0.37
		0.425	200	3.46E−3	4.48E−6	0.24
		1.7	300	3.46E−3	3.19E−6	0.54
		1.7	250	3.46E−3	3.04E−6	0.69
		1.7	200	3.46E−3	3.44E−6	0.73
		1.7	150	3.46E−3	3.36E−6	0.82
		1.7	100	3.46E−3	3.61E−6	1.19
		1.7	50	3.46E−3	1.18E−5	3.00

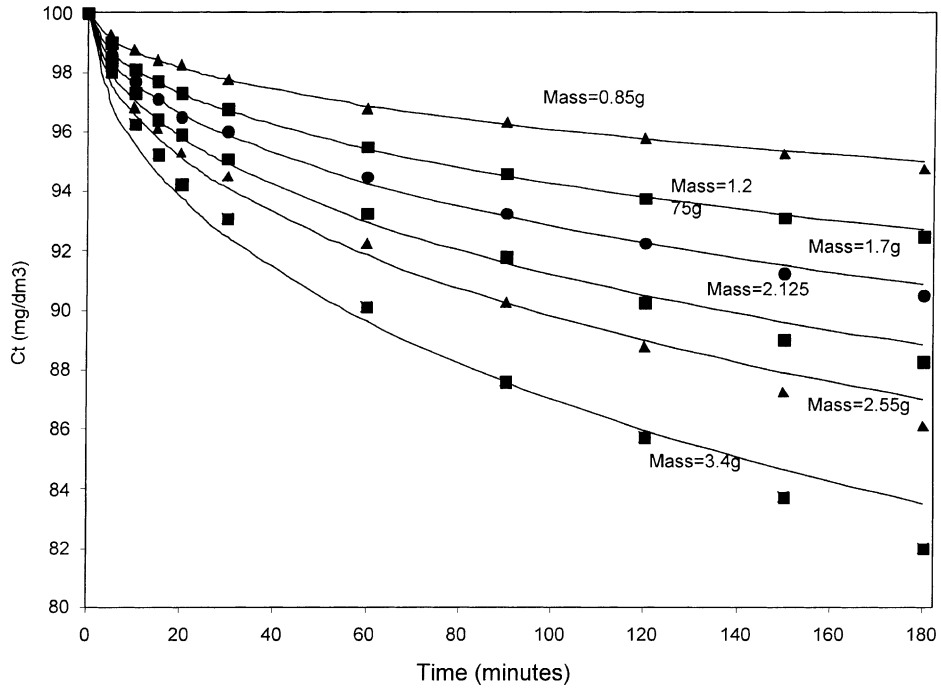

Fig. 6. Effect of adsorbent mass for AB25 on pith by using the searched best individual D_{eff} values.

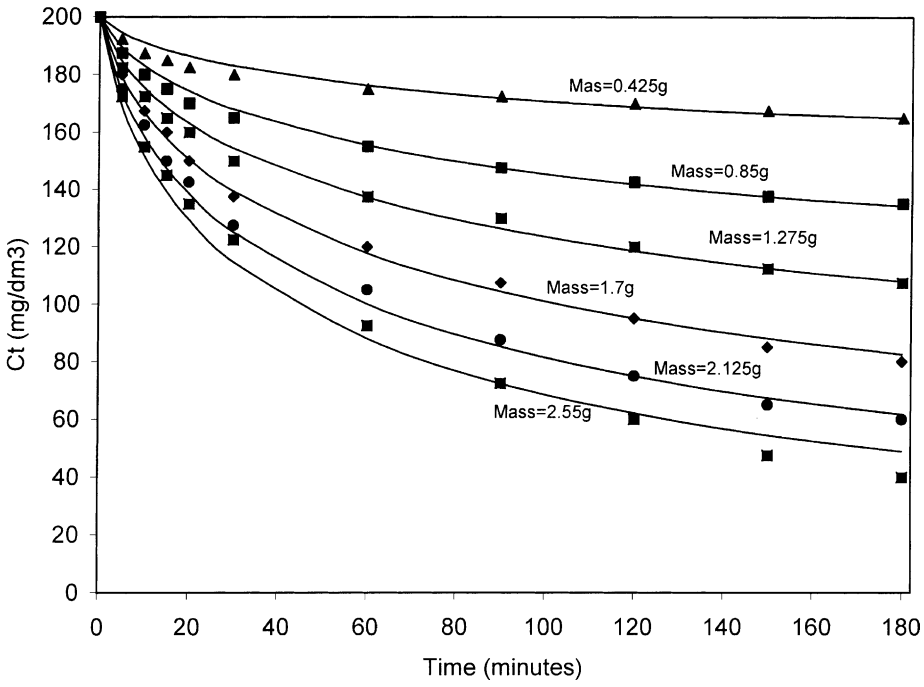

Fig. 7. Effect of adsorbent mass for BB69 on pith by using the searched best individual D_{eff} values.

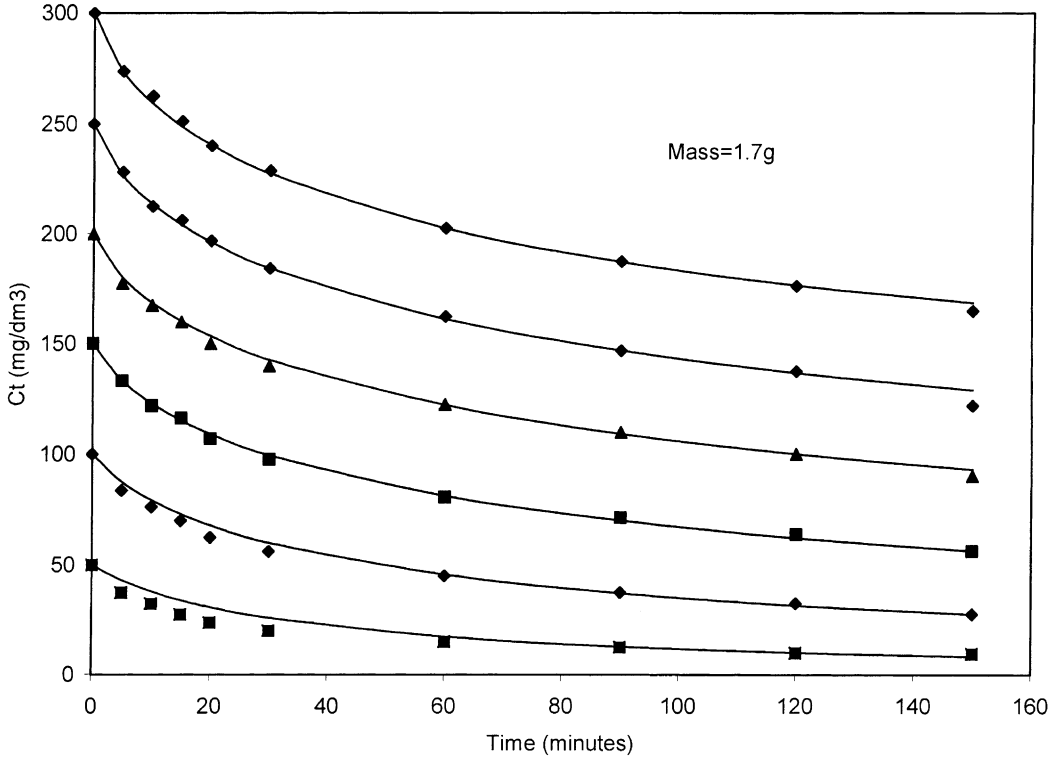

Fig. 8. Effect of initial concentration for BB69 on pith by using the searched best individual D_{eff} values.

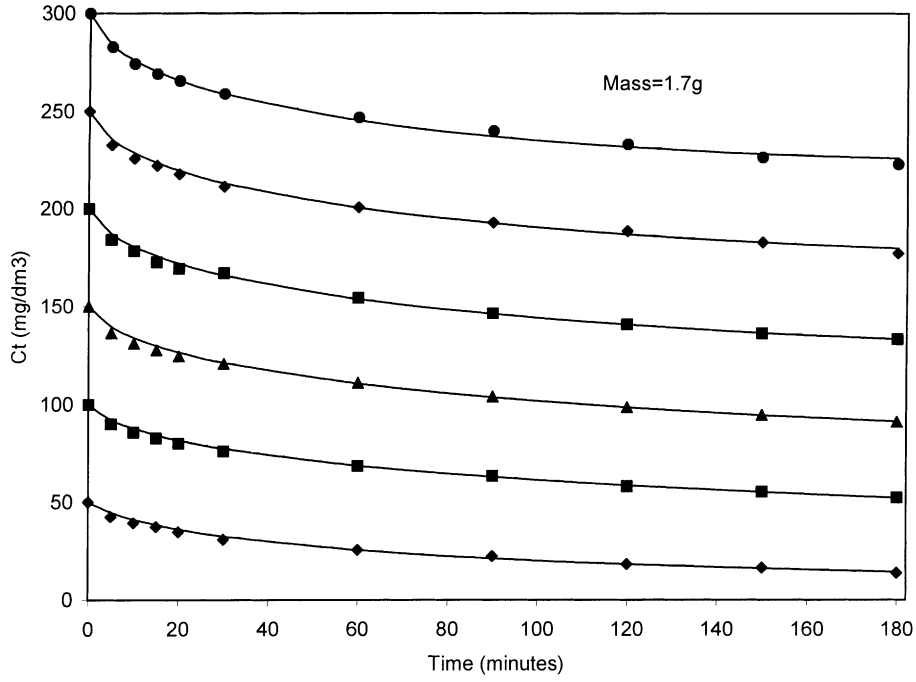

Fig. 9. Effect of initial concentration for BR22 on pith by using the searched best individual D_{eff} values.

Table 9
Correlation constants for D_{eff}

Dye	a	b	r^2	c	d	r^2
AB25	8.89E−6	−0.65	0.979	4.09E−7	−0.204	0.973
ARll4	5.25E−6	−0.415	0.915	7.47E−7	−0.234	0.968
BB69	1.59E−3	−1.00	0.974	8.18E−6	0.175	0.915
BR22	1.23E−5	−0.241	0.906	3.01E−6	−0.465	0.994

was decided to correlate D_{eff} as functions of the systems variables using equations of the following form:

$$D_{eff} = aC_0^b \quad (4)$$

$$D_{eff} = cS^d \quad (5)$$

The values of a, b, c and d are shown in Table 9.

These correlations have sufficiently high correlation coefficients to be used in the optimization studies for second stage batch sorber design.

3.4. Optimization

The four systems to be optimized are shown in Table 10; the sorbent masses, solution volumes, initial solute concentrations are presented in the table.

The following parameters for the dyestuffs on pith two-stage batch adsorber systems are not changed in the optimization procedure. For the first optimization study, the fixed values are (we designate this Case 1).

1. The adsorbent weight (S_1, S_2) in each batch adsorber.
2. The agitation speed in each batch adsorber (400 rpm).
3. The initial solid-phase concentration is zero, i.e. each batch adsorber uses fresh adsorbent.
4. Equilibrium solid-phase concentration q_e is in equilibrium with the initial liquid phase concentration of each stage, and calculated by the Langmuir equation. Let t_1, t_2 and t (here, $t = t_1 + t_2$) be the contact time in the first adsorber, the second adsorber and the two-stage batch adsorber system, respectively. The following objective function is taken to perform the optimization:

Table 10
Four two-stage batch adsorption systems to be optimized

System (sorbate–sorbent)	Sorbent mass (g)		V (dm^3)	C_0 (mg/dm^3)	C_2 (mg/dm^3)
	S_1	S_2			
AB25–pith	3.4	3.4	1.7	79	40
AR114–pith	3.4	3.4	1.7	100	40
BB69–pith	1.7	1.7	1.7	300	40
BR22–pith	2.125	2.125	1.7	200	40

$$\text{minimize } t(C_{0,2}) \tag{6}$$

This model to be solved consists of highly non-linear equations. In order to make the model easier to be solved, an initialization and the feasibility region of $C_{0,2}$ can be determined prior to the optimization. The limits are very important to the optimization problem. If reasonable limits of the variable ($C_{0,2}$) are chosen, the solution time can be significantly reduced.

The basic assumptions to determine the valid range of initial concentration of the second stage are:

1. The adsorbent weight and species of the first stage are the same as for the second stage to maintain S/V constant in each stage.
2. The equilibrium concentration of solid-phase (adsorbent phase) used in the first and the second stage are the same (monolayer assumption), because this value is used in the mass transfer model to provide a constant surface concentration which enables the rapid analytical solution to be obtained.

The procedure for determining the upper ($C_{\max}$) and lower ($C_{\min}$) bound of $C_{0,2}$ has been evaluated using the following procedure.

3.4.1. Lower limit of $C_{0,2}$

For the second stage, the capacity factor C_h must be less than or equal to 1.0 according to the SCM model, i.e.

$$\frac{Sq_e}{VC_{\min}} \leq 1.0 \tag{7}$$

Let,

$$\frac{Sq_e}{V} = C_{\min 1} \tag{8}$$

Another limit is determined when the first stage is saturated, i.e.

$$VC_0 - VC_{\min} \leq Sq_e \tag{9}$$

Let,

$$\frac{VC_0 - Sq_e}{V} = C_{\min 2} \tag{10}$$

From Eqs. (8) and (10), we obtain

$$C_{0,2} \geq C_{\min 1} \tag{11}$$

$$C_{0,2} \geq C_{\min 2} \tag{12}$$

Inequalities (14) and (15) are equivalent to

$$C_{0,2} \geq \max[C_{\min 1}, C_{\min 2}] \tag{13}$$

So, the lower limit of initial concentration of the second stage is as follows:

$$(C_{0,2})_{\text{lower}} = \max[C_{\min 1}, C_{\min 2}] \tag{14}$$

3.4.2. Upper limit of $C_{0,2}$

For the second stage which must meet the design limit C_2, the maximum value of initial concentration ($C_{0,2}$) is subjected to the limit

$$VC_{\max} - VC_2 \leq Sq_e \tag{15}$$

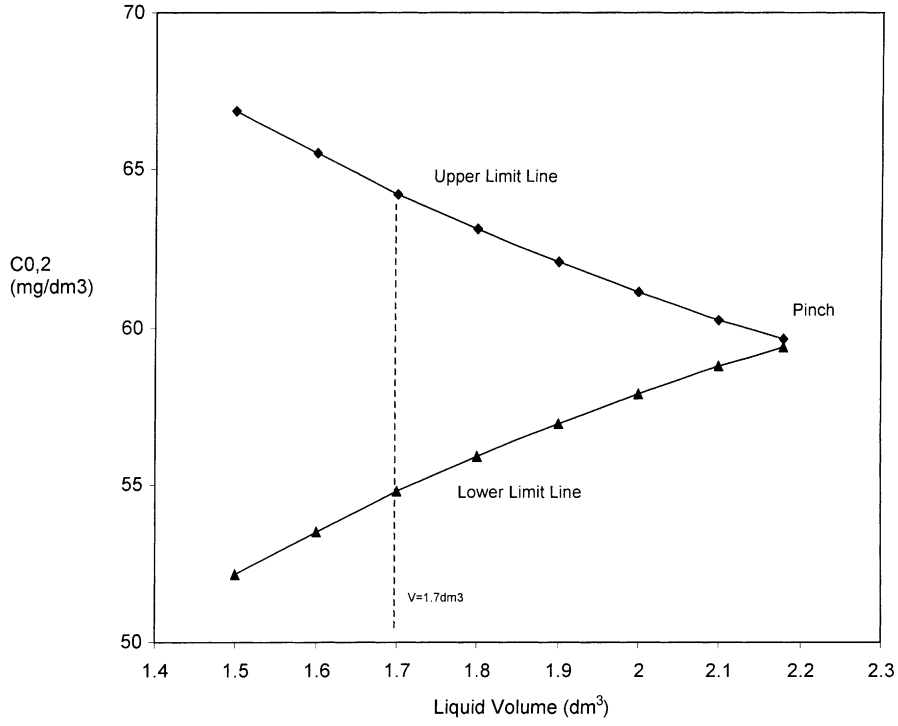

Fig. 10. Upper and lower limits of $C_{0,2}$ for AB25 on pith.

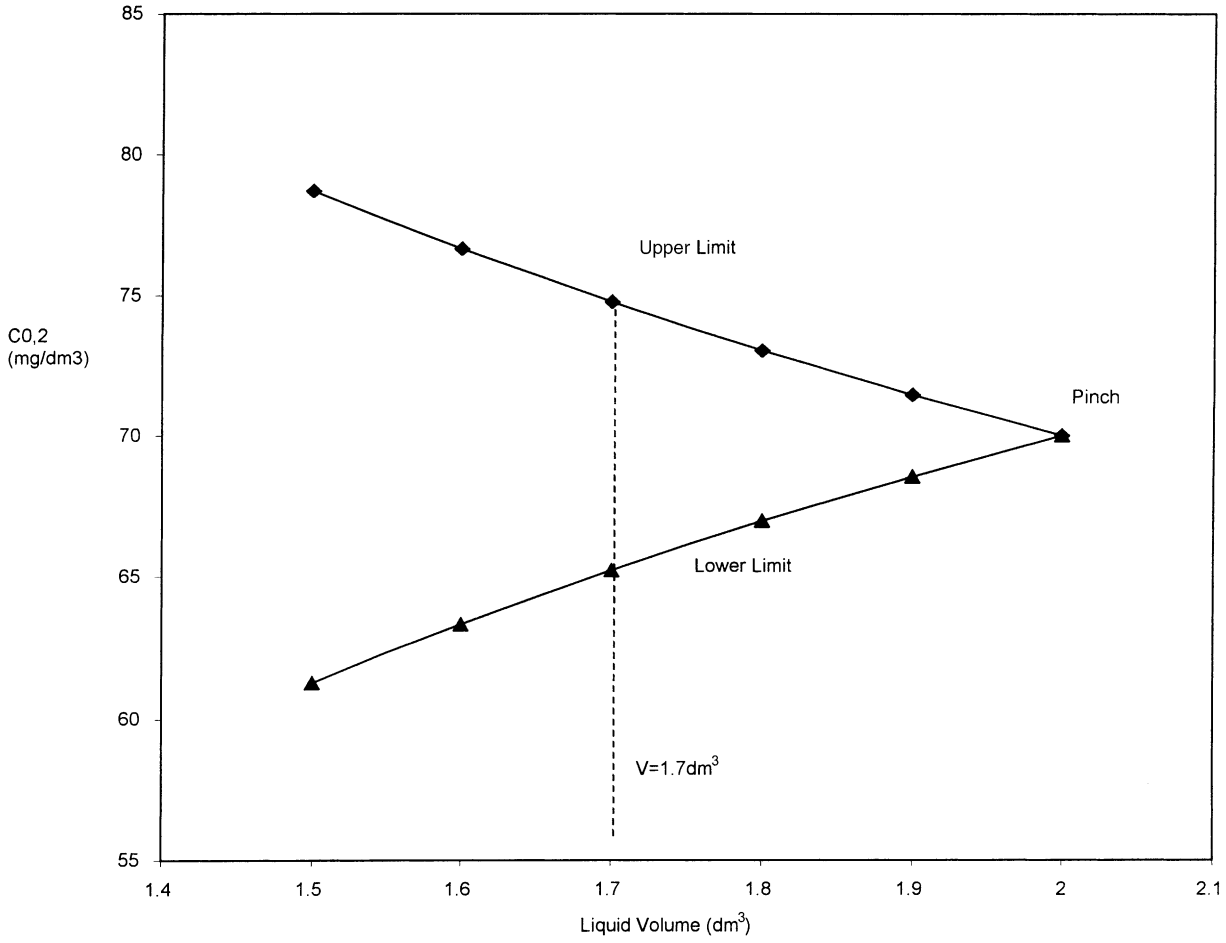

Fig. 11. Upper and lower limits to of $C_{0,2}$ for AR114 on pith.

That is

$$C_{\max} \leq \frac{Sq_e + VC_2}{V} = \frac{Sq_e}{V} + C_2 \tag{16}$$

Let,

$$C_{\max 1} = \frac{Sq_e}{V} + C_2 \tag{17}$$

For the first stage, the maximum value of $C_{0,2}$ must be less than its initial concentration (C_0). So, the upper limit of $C_{0,2}$ is as follows:

$$(C_{0,2})_{\text{upper}} = C_{\max 1} < C_0 \tag{18}$$

The upper and lower bound of the four systems at different initial liquid volumes are shown in Figs. 10–13. By knowing these bounds, the initial value of $C_{0,2}$ can be calculated using the following equation:

$$C_{0,2} = 0.5(C_{\min} + C_{\max}) \tag{19}$$

$$C_{\max} \geq C_{0,2} \geq C_{\min} \tag{20}$$

Fig. 10 shows the upper and lower limits of the feed concentration to the second stage adsorber, $C_{0,2}$, and the optimum values when V changes from 1.5 to 2.0 dm^3. The optimal values of $C_{0,2}$ are equal to the lower limit values when V is greater than or equal to 2.0 dm^3, which means the first stage must be saturated when V is greater than or equal to 2.0 dm^3 in order to meet the condition. This we term the "pinch point" of the batch adsorber system when the upper limit value of $C_{0,2}$ is equal to the lower limit value of $C_{0,2}$. This implies that it is impossible to meet the design limit when the value of $C_{0,2}$ is below it.

3.4.3. Results of Case 1

The tradeoffs between t_1 and t_2 and the optimum $C_{0,2}$ of the four systems are shown in Figs. 14–17. The minimum contact time and optimal initial concentration of second stage are also listed in Table 11.

3.4.4. Optimization of the two-stage batch system in Case 2

The following parameters of the two-stage batch adsorber system are not changed in the optimization procedure. They are (we designate in this Case 2).

The points (2)–(4) are the same as Case 1, and the total adsorbent masses (1) in the first stage and second stage are 6.8, 3.027, 2.01 and 4.25 g for the four systems shown

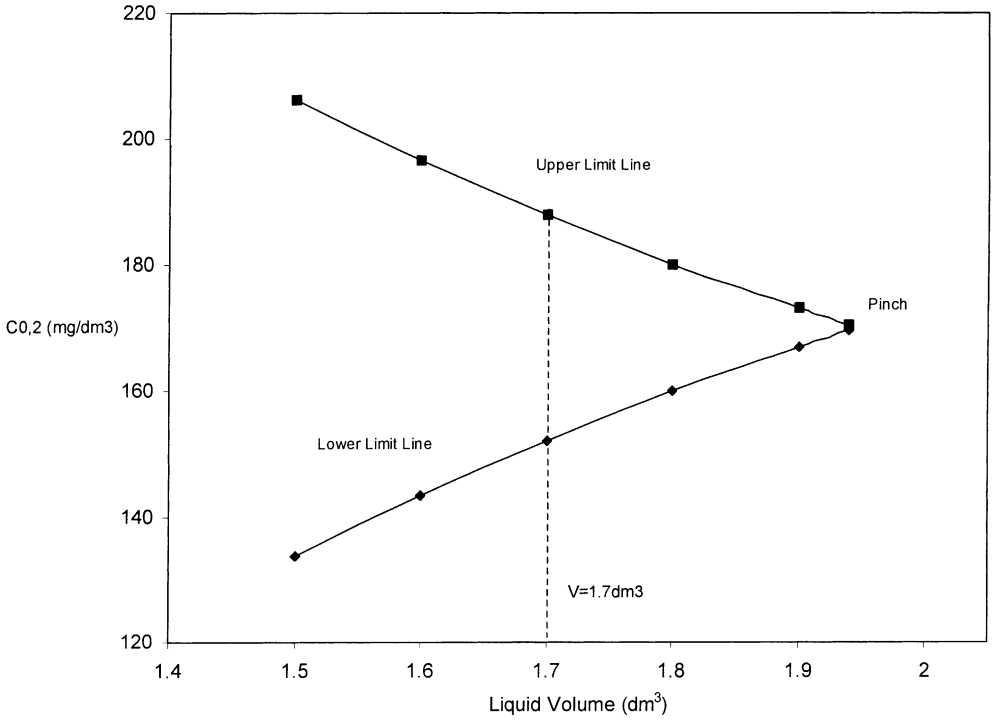

Fig. 12. Upper and lower limits of $C_{0,2}$ for BB69 on pith.

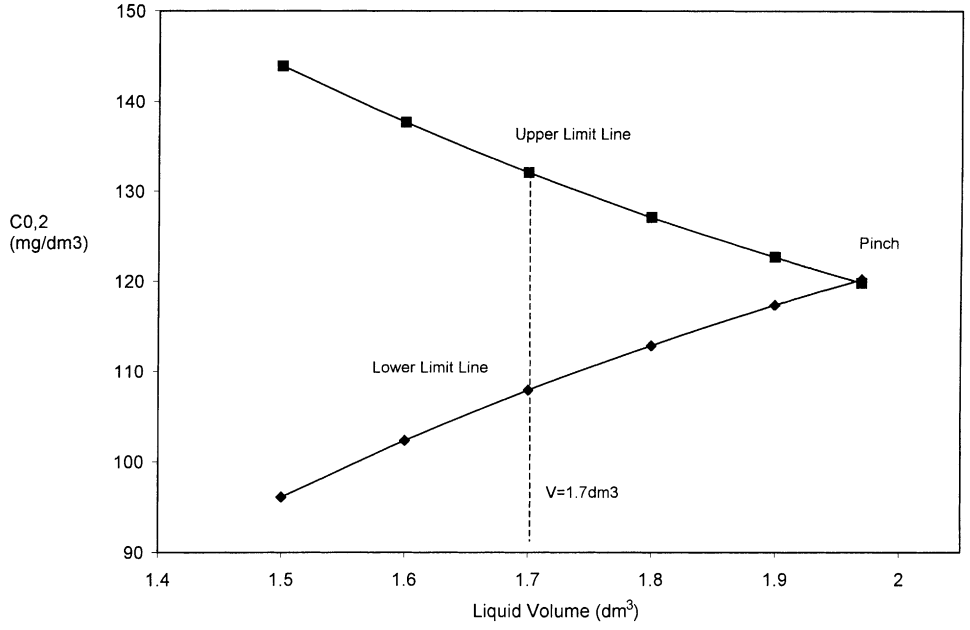

Fig. 13. Upper and lower limits of $C_{0,2}$ for BR22 on pith.

in Table 12, respectively. The adsorbent weight in the first stage, S_i, will be changed as a variable.

The contact times are t_1, t_2 and t (here, $t = t_1 + t_2$) in the first adsorber, the second adsorber and the two-stage batch adsorber system, respectively. The following objective function is taken to perform the optimization

$$\text{minimize } t(S_1, C_{0,2}) \tag{21}$$

$$\text{subject to } C_{\min} \leq C_{0,2} \leq C_{\max} \tag{22}$$

$$S_1 + S_2 = 6.8 \text{ (systems 1 and 2)} \tag{23}$$

$$S_1 + S_2 = 3.4 \text{ (system 3)} \tag{24}$$

$$S_1 + S_2 = 4.25 \text{ (system 4)} \tag{25}$$

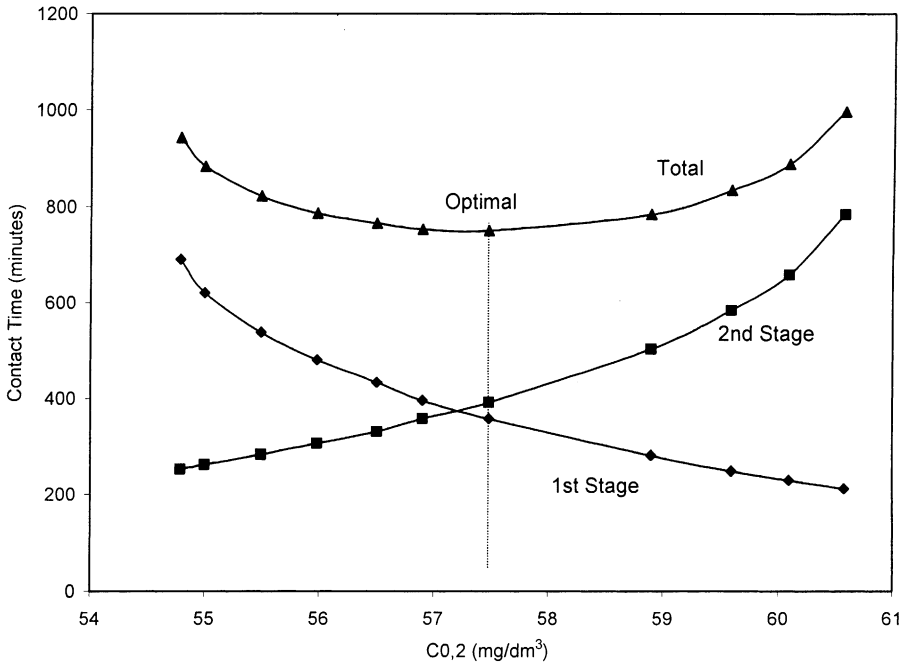

Fig. 14. Optimal contact time for AB25 on pith.

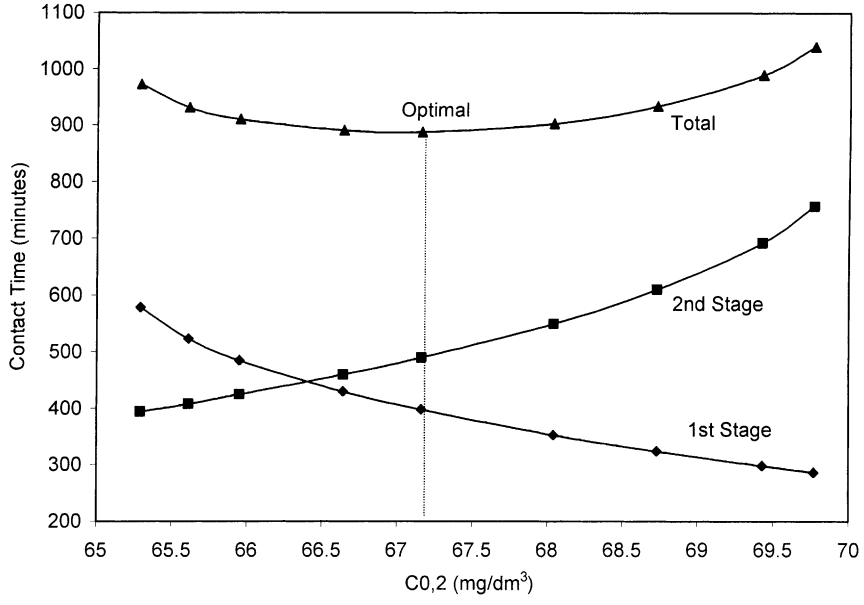

Fig. 15. Optimal contact time for AR114 on pith.

Table 11
Optimization results of four two-stage batch adsorption systems at Case 1

System (sorbate–sorbent)	Sorbent mass (g)		V (dm^3)	C_0 (mg/dm^3)	C_2 (mg/dm^3)	$C_{0,2}$ (mg/dm^3)	Optimal contact time (min)
	S_1	S_2					
AB25–pith	3.4	3.4	1.7	79	40	57.48	751
AR114–pith	3.4	3.4	1.7	100	40	67.16	888
BB69–pith	1.7	1.7	1.7	300	40	154.82	541
BR22–pith	2.125	2.125	1.7	200	40	112.95	959

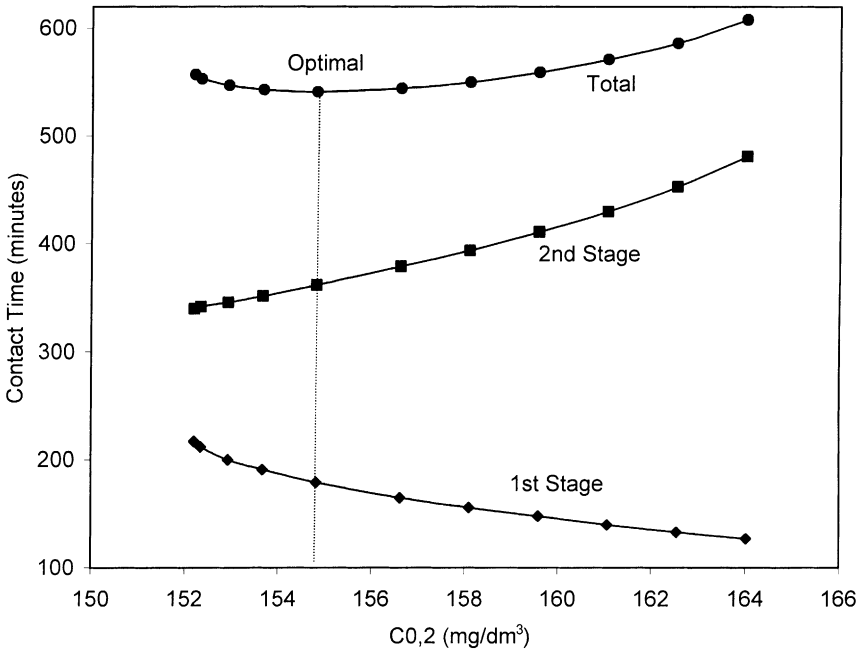

Fig. 16. Optimal contact time for BB69 on pith.

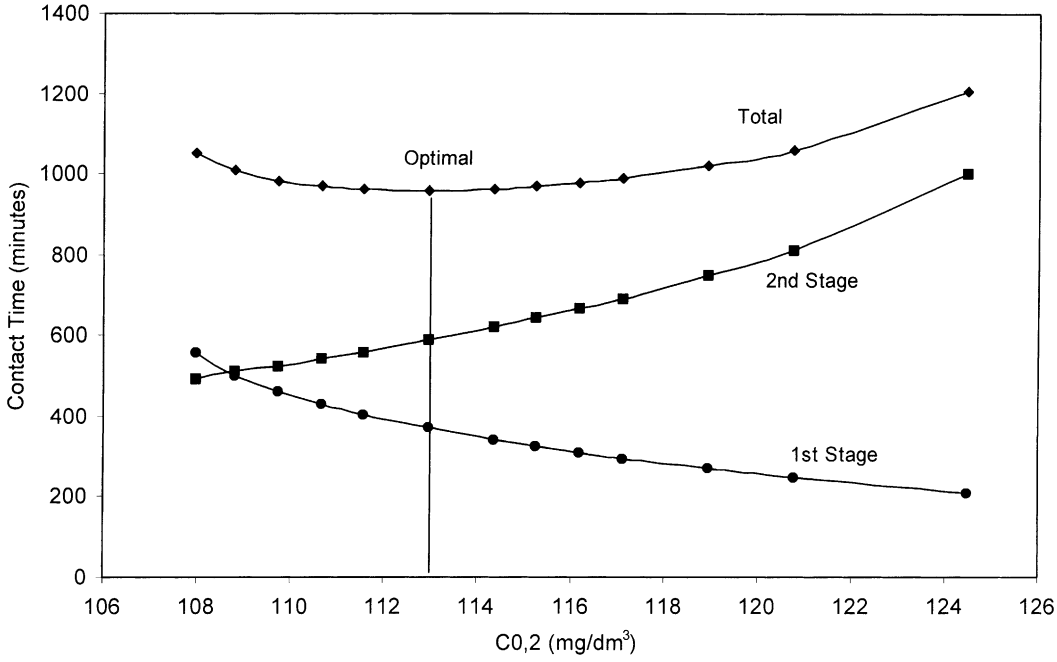

Fig. 17. Optimal contact time for BR22 on pith.

Table 12
Optimization results of four two-stage batch adsorption systems at Case 2

System (sorbate–sorbent)	Sorbent mass (g)		V (dm^3)	C_0 (mg/dm^3)	C_2 (mg/dm^3)	$C_{0,2}$ (mg/dm^3)	Optimal contact time (min)
	S_1	S_2					
AB25–pith	6.8	0	1.7	79	40	40	533
AR114–pith	3.27	3.53	1.7	100	40	68.35	888
BB69–pith	2.01	1.39	1.7	300	40	129.78	539
BR22–pith	4.25	0	1.7	200	40	40	672

The minimum contact time and optimal S_i and $C_{0,2}$ are shown in Table 12.

The adsorbent weight in two batch absorbers is a key parameter for the optimization problem.

4. Conclusions

1. The equilibrium isotherms of four adsorption systems of dyestuffs (AB25, AR114, BB69 and BR22) on pith can be formulated precisely by the Langmuir equation.
2. The film-pore diffusion model with a constant effective diffusion coefficient, model 1, is simple and fast and can be used in predicting concentration decay curves of dyestuffs (AB25, AR114, BB69 and BR22) on pith adsorption systems except for few cases with very low initial concentration.
3. The film-pore diffusion model with individual effective diffusion coefficient for each initial concentration (model 2) can be used in modeling mass transport behavior of dyestuffs (AB25, AR114, BB69 and BR22) on pith for a wide range of initial concentrations. The effective diffusion coefficient in model 2 can be expressed as a function of adsorbate initial concentration.
4. An optimization methodology of a two-stage batch adsorber system taking minimum contact time as the objective function, the initial concentration of the second stage and/or adsorbent weight as variable(s) has been developed. The optimization results are useful for optimal design of batch processes.
5. There are different minimum values of the contact time for the optimizations of a two-stage batch adsorber system at different process conditions. There is a significant difference among these optimal results (minimum contact time changes from 751 to 533 min for the AB25–pith system, 959 to 672 min for the BR22–pith system). So, it is very important that the optimal distribution of adsorbent weight in two stages.
6. There is always a "pinch point" for the optimization of a two-stage batch adsorber system, or namely the design limit. It is impossible or possible to meet the design specification when the initial concentration value of second stage surpasses or is below the "pinch point".

References

[1] F.J. Edeskuty, N.R. Amundson, J. Phys. Colloid Chem. 56 (1952) 148.
[2] F.J. Edeskuty, N.R. Amundson, J. Phys. Colloid Chem. 44 (1952) 1698.
[3] P.R. Kasten, N.R. Amundson, Ind. Eng. Chem. 44 (1952) 1704.
[4] P.R. Kasten, L. Lapidus, N.R. Amundson, J. Phys. Chem. 56 (1952) 683.
[5] F.A. Di Giano, W.J. Weber Jr., J. Water Pollut. Control Fed. 45 (1973) 713.
[6] T.W. Weber, Can. J. Chem. Eng. 56 (1978) 187.
[7] I. Abe, K. Haygashi, T. Hirashima, Colloids Surf. 8 (1984) 315.
[8] G. McKay, B.A. Al Duri, Chem. Eng. Sci. 43 (1988) 1133.
[9] M.R.L. Glover, B.D. Young, A.W. Bryson, Int. J. Miner. Process 30 (1990) 217.
[10] B.D. Young, J.D. Le Roux, A.W. Bryson, Hydrometallurgy 26 (1991) 395.
[11] G. McKay, M.J. Bino, A. Altemimi, Water Res. 20 (1986) 435.
[12] H. Yoshida, T. Kataoka, Chem. Eng. J. (Lausanne) 41 (1989) 811.
[13] S. Yagi, D. Kunii, Chem. Eng. Sci. 16 (1961) 372.
[14] O. Levenspiel, Chemical Reaction Engineering, Wiley, New York, 1962.
[15] R.G. Lerch, D.A. Rathowsky, Optimum allocation of adsorbent in stagewise adsorption operation, Ind. Eng. Chem. Fundam. 6 (1067) 308.
[16] G. McKay, S.J. Allen, Surface mass transfer processes using peat as an adsorbent for dyestuffs, Can. J. Chem. Eng. 58 (1980) 521.
[17] H. Spahn, E.U. Schlunder, Chem. Eng. Sci. 30 (1975) 529.
[18] W. Fritz, W. Merk, E.V. Schlunder, Competitive adsorption of two dissolved organics onto activated carbon-II, Chem. Eng. Sci. 36 (1981) 731.
[19] W. Merk, W. Fritz, F.U. Schlunder, Competitive adsorption of two dissolved organics onto activated carbon-III, Chem. Eng. Sci. 36 (1980) 743.
[20] G. McKay, The adsorption of dyestuffs from aqueous solution using activated carbon. Analytical solution for batch adsorption based on external mass transfer and pore diffusion, Chem. Eng. J. 27 (1983) 187.
[21] G. McKay, M. El-Geundi, M.M. Nassar, Pore diffusion during the adsorption of dyes onto bagasse pith, Trans. IChemE B: Process Safety Environ. Protect. 74 (1996) 277.
[22] W. Holl, H. Sontheimer, Ion-exchanger kinetics of the protonation of weak acid ion-exchange resins, Chem. Eng. Sci. 32 (1977) 755.
[23] A. Fernandez, A. Rodrigues, M. Diaz, Kinetics mechanism in ion-exchange processes, Chem. Eng. J. 57 (1995) 17.
[24] F. Helfferich, Models and physical reality in ion-exchange kinetics, React. Polym. 13 (1990) 191.
[25] N. Pinto, E. Graham, Application of the shrinking core model for predicting protein adsorption, React. Polym. 5 (1987) 49.
[26] E. Arevalo, M. Rendueles, A. Fernandez, A. Rodrigues, M. Diaz, Uptake of copper and cobalt in a complexing resin: shrinking-core model with two reaction fronts, Sep. Purif. Technol. 13 (1998) 37.
[27] H. Komiyama, J.M. Smith, Surface diffusion in liquid filled pores, AIChE J. 20 (1974) 1110.
[28] D. Do, R.G. Rice, On the relative importance of pore and surface diffusion in nonequilibrium adsorption rate processes, Chem. Eng. Sci. 42 (1987) 2269.
[29] I. Neretnieks, Adsorption of components having a saturation isotherm, Chem. Ing. Technol. 46 (1974) 781.
[30] G. McKay, Analytical solution using a pore diffusion model for a pseudo-irreversible isotherm for the adsorption of basic dye on silica, AIChE J. 30 (1984) 692.
[31] S.M. Saad, A.M. Nasser, M.T. Zimaity, H.F. Abdel-Magad, J. Oil Colour Chem. Assoc. 61 (1978) 43.
[32] T. Furusawa, J.M. Smith, Fluid particle and intraparticle mass transfer rates in slurries, Ind. Eng. Chem. Fundam. 12 (1973) 197.
[33] T. Furusawa, J.M. Smith, Diffusivities from dynamic data, AIChE J. 19 (1973) 401.
[34] G. McKay, S.J. Allen, Single resistance mass transfer models for the adsorption of dyes on peat, J. Sep. Proc. Technol. 4 (1983) 1.
[35] G. McKay, S.J. Allen, Surface mass transfer processes using peat as an adsorbent for dyestuffs, Can. J Chem. Eng. 62 (1984) 340.